

VANDERBILT UNIVERSITY

DEPARTMENT OF CHEMICAL AND BIOMOLECULAR ENGINEERING

Active Motion of Janus Particles in AC Electric Fields

By:

Behrouz Behdani

Proposal submitted to:

Prof. Carlos A. Silvera Batista

Assistant Professor of Chemical and Biomolecular Engineering
Chair

Prof. Justus Ndukaife

Assistant Professor of Electrical Engineering

Prof. Kane Jennings

Professor of Chemical and Biomolecular Engineering

Prof. Matthew Lang

Professor of Chemical and Biomolecular Engineering

Prof. Paul Laibinis

Professor of Chemical and Biomolecular Engineering

Motivation

One of the most interesting developments in the microfluidics area is the emergence of artificial active systems. Inspired by swarming motion of living organisms in the nature, active particles use the stored energy in the environment to initiate self propulsion. These microrobots can perform complicated tasks such as selective cargo transport (Park et al. 2021, Boymelgreen et al. 2016), drug delivery (Niu and Palberg 2018) and fluid actuation (Shields and Velev 2017). Successful use of active particles in these systems depends on the capability of these particles to travel in the biological environments, many of which are more complex than laboratory experimental setups. Different approaches have been used to control and navigate the artificial active particles. They include chemical reaction (Choudhury et al. 2017), thermally-driven actuation (Chen et al. 2018) and applying external forces (Takatori and Brady 2016, Demirörs et al. 2018). In all of these applications, active particles move due to a local gradient . The local gradient originates from the broken symmetry around the particle. The emerging issue is that the active motion of the particle is randomized due to the rotational diffusion at higher time-scales. To achieve control over particle's propulsion, the active motion should be programmed by utilizing a unique property of the system. AC electrokinetics has the potential to program the self-propulsion of the particles. In these systems, the motion is caused by the interaction of particles with each other and the external field. One way to achieve the broken symmetry, required for active motion, is to use Janus particles. Metallodielectric Janus particles (JPs) are microparticles with two halves, each possessing distinct physical properties (Walther and Müller 2008). From the standpoint of electrical properties, one half is dielectric with low surface conductivity while the other half, is a highly conductive metal. Previous works in the literature show successful application of these colloidal systems for electroporation of bacteria and cargo transport. The advantage of using electric field in these systems is the simplicity of the process as the controlling factor is only the frequency and amplitude of external field and it does not require complex geometries. Despite important advances in the application (Boymelgreen et al. 2017, 2018), the explanation of physics which govern the motion of the particles is not clear. Therefore, a systematic study is needed, which can correlate the active motion of JPs to the dielectric properties of the system. Finding this relation, can also help to connect the self propulsion of a single particle to the collective dynamics of highly concentrated sample of particles, which is the case in realistic biological environments.

In this project, we investigate the collective dynamics and the self propulsion of metallodielectric Janus particles in the presence of AC electric field. **Our central hypothesis is that engineering charge relaxation times of colloidal particles is the key to control the self propulsion and the collective dynamics of particles in AC fields.** Our hypothesis was formulated based on our preliminary experimental and simulation results. We will test our hypothesis by pursuing the following aims:

- **Aim 1:** *Investigating the electric polarizability of metallodielectric Janus spheres and ellipsoids in electrolyte solution.* Electrorotation measurements and numerical simulation in COMSOL Multiphysics can quantify the effect of the particle's structure and the medium on the polarizability of particles.
- **Aim 2:** *Engineering self propulsion of particles through the manipulation of polarizability.*

The relation between polarizability and self propulsion of a single particle is to be established.

- **Aim 3:** *Control collective dynamics of active colloids in AC field.* The effect of concentration and domain confinement on the collective dynamics of particles will be studied.
- **Aim 4:** *Light driven motion of self propelled Janus particles in the presence of AC field.* Light activated colloids are to be used for initiating self propulsion and collective dynamics in the suspension.

Methods

Before discussing each aim in detail, we discuss all the common theoretical and experimental methods which are used to achieve the goal of the proposal. Specifically, we elaborate on *particle and setup fabrication* and, *modeling of electrokinetics*.

Particle and setup fabrication

Janus particles include monolayer of titanium on the silica spheres. Silica spheres with diameter of 3.66 micron are cleaned through cycle of centrifugation-solvent exchange and then resuspension. Then, monolayer of silica is deposited by using convection self assembly with the speed of 8 mm/s. Before the deposition, the glass slide is cleaned and sonicated sequentially in acetone , isopropanol and DI water for 10 minutes and then treated in UV Ozone for 10 minutes. Titanium layers (5, 15 and 35 nm) and SiO₂ (20 nm) are deposited on the silica sphere by using electron beam physical deposition. Additional silica layer will give particles a surface charge which prevents attraction of particles to the surface. The experimental setup includes the electrode chamber, the confocal microscope and the electric field generator. For generating the electric field, the electrodes are connected to a two-phase channel function generator. The frequency range is between 100 Hz and 20 MHz and particle rotations are captured using a 20X, 0.75 NA air objective.

Modeling of electrokinetics

When subjected to an oscillating electric field, $E = \text{Re} [\tilde{E} e^{i\omega t}]$, a particle acquires a time-changing dipole moment, given by $p = \text{Re} [\tilde{p} e^{i\omega t}]$. In these expressions, \tilde{E} and \tilde{p} represent the phasors for the electric field and the dipole moment, while $\omega = 2\pi f$ represents the angular frequency. The interaction between an induced dipole and a rotating field leads to a torque, ($T_e = p \times E$). (Pethig 2017) For JPs, the induced dipole moment can be decomposed into components parallel and perpendicular to the equator,

$$\tilde{p} = 4\pi\epsilon r^3 [A(\omega)\tilde{E}_x + B(\omega)\tilde{E}_y]; \quad (1)$$

ϵ is the permittivity of the medium, while $A(\omega)$ and $B(\omega)$ are the nondimensional complex polarizabilities parallel and perpendicular to the equator, respectively; r is the particle's radius. In an electrorotation experiment, the quantity of interest is the time-averaged torque in a rotating electric field, $\tilde{E} = E_0(e_x + ie_y)$, which is given by:

$$\tau_e = \frac{1}{2}\text{Re} [\tilde{p} \times \tilde{E}^*] = -2\pi\epsilon r^3 E_0^2 \cdot \text{Im} [A(\omega) + B(\omega)] e_z, \quad (2)$$

after replacing values for \tilde{p} and the complex conjugate of the electric field phasor, \tilde{E}^* .

At low Reynolds numbers, inertia is negligible and the viscous torque, $T_v = 8\pi\eta R^3\Omega e_z$, balances the electrical torque, thus producing an expression that correlates the measured angular velocity (Ω) with the imaginary component of the polarizability,

$$\Omega = -\frac{\varepsilon E_0^2}{4\eta} \cdot \text{Im} [A(\omega) + B(\omega)]. \quad (3)$$

E_0 and η stand for the magnitude of the electric field and the viscosity of the fluid, respectively. To find the correlation between polarizability and angular velocity, at first, we solved Poisson-Nernst-Planck equations to find the distribution of potential and concentration in the medium and Laplace equation to derive the distribution of potential inside the particle. Janus particle includes a silica sphere, one layer of metal on one half and another layer of silica on the top of the metal. Our analysis follows a formalism similar to those in references (Miloh and Nagler 2020) (Zhao 2011), and in particular, the one developed by Zhao.(Zhao 2011) The electric potential in the liquid domain follows the PNP equations:

$$\nabla^2 \Phi_1 = -\frac{e(C_+ - C_-)}{\varepsilon}, \quad (4)$$

$$\frac{\partial C_+}{\partial t} = -\nabla \cdot J_+ \quad \text{with} \quad J_+ = -D_+ \nabla C_+ - C_+ \mu_+ \nabla \Phi_1 + C_+ V, \quad (5)$$

$$\frac{\partial C_-}{\partial t} = -\nabla \cdot J_- \quad \text{with} \quad J_- = -D_- \nabla C_- - C_- \mu_- \nabla \Phi_1 + C_- V, \quad (6)$$

where, C_{\pm} , Φ , and e are the concentration of ions, the electrical potential, and elementary charge. The mobilities are given by the Einstein-Smoluchowski equation, $\mu_{\pm} = D_{\pm} e z_{\pm} / k_B T$. D_{\pm} and $k_B T$ are the diffusivity of ions and the thermal energy, while J_{\pm} represents the flux of ions due to diffusion, migration and convection. As a first approximation, we will ignore the contributions from hydrodynamics to the flux of ions. Boundary conditions are needed to solve this set of coupled equations. At the far field, the potential equals the external potential (Φ_e), and the concentration of ions equals the bulk concentration (C_b). At the particle-liquid interface, the continuity of potential, the continuity of electric field displacement, and zero flux of ions applies:

$$\Phi_1 = \Phi_2, \quad (7)$$

$$\varepsilon_1 \frac{\partial \Phi_1}{\partial n} - \varepsilon_2 \frac{\partial \Phi_2}{\partial n} = \Gamma_s, \quad (8)$$

$$n \cdot J_- = 0, \quad n \cdot J_+ = 0. \quad (9)$$

Γ_s represents the permanent surface charge. The equations are solved in dimensionless form using the particle radius (r) as the length scale, $k_B T/e$ —thermal voltage (Φ_T)—as the potential scale, C_b as the concentration scale, and r^2/D_+ as the time scale. The scales for the electric charge, the mass flux and the velocity are $\varepsilon_1 k_B T / er$, $D_+ C_b / r$, and $\varepsilon_1 k_B^2 T^2 / \eta e^2 r$. The diffusivities of the ions are scaled by D_+ . The hat above a variable stands for its dimensionless form. Under a weak external field, electron transfer is unlikely to take place at the particle-liquid interface, and the double layer is only slightly perturbed. Consequently, solutions to the model are pursued by writing perturbation expansions of the form,

$$\hat{C}_{\pm} = \hat{C}_{\pm}^0 + \delta \hat{C}_{\pm}^1 e^{-i\hat{\omega}\hat{t}}, \quad (10)$$

$$\hat{\Phi} = \hat{\Phi}^0 + \delta\hat{\Phi}^1 e^{-i\hat{\omega}\hat{t}}. \quad (11)$$

\hat{C}_\pm^1 and $\hat{\Phi}^1$ represent small perturbations from the respective equilibrium values, \hat{C}_\pm^0 and $\hat{\Phi}^0$. In these equations, δ denotes the ratio between the external electric field and the field associated with the equilibrium double layer (Zhao 2011). By rewriting the PNP equations in terms of the new variables and neglecting the nonlinear terms in δ , the problem can be solved in two parts. First, the problem for the equilibrium double layer is,

$$\nabla^2 \hat{\Phi}_1^0 = -\frac{\hat{C}_+^0 - \hat{C}_-^0}{2\hat{\lambda}^2}, \quad 0 = -\nabla \cdot \hat{J}_\pm, \quad (12)$$

with boundary conditions

$$0 = \hat{J}_\pm, \quad \hat{\Phi}_1^0 = \hat{\zeta} \quad \text{at} \quad \hat{r} = 1. \quad (13)$$

The dimensionless Debye length ($\hat{\lambda}$) is defined as $\hat{\lambda} = \frac{1}{r} \left(\frac{\varepsilon \varepsilon_0 k_B T}{2C_b e^2} \right)^{1/2}$. $\hat{\zeta}$ represents the scaled zeta potential. The problem describing the perturbations caused by the imposed field is

$$i\omega \hat{C}_\pm^1 + \nabla \cdot [\hat{D}_\pm \nabla \hat{C}_\pm^1 + z_\pm \hat{D}_\pm \hat{C}_\pm^1 \nabla \hat{\Phi}_1^0 + z_\pm \hat{D}_\pm \hat{C}_\pm^0 \nabla \hat{\Phi}_1^1] = 0, \quad (14)$$

$$\nabla^2 \hat{\Phi}_1^1 = -\frac{\hat{C}_+^1 - \hat{C}_-^1}{2\hat{\lambda}^2} \quad (15)$$

$$\nabla^2 \hat{\Phi}_2^1 = 0, \quad (16)$$

with boundary conditions at the particle surface

$$\hat{\Phi}_1^1 = \hat{\Phi}_2^1, \quad (17)$$

$$\frac{\partial \hat{\Phi}_1^1}{\partial \hat{n}} - \varepsilon_r \frac{\partial \hat{\Phi}_2^1}{\partial \hat{n}} = 0, \quad (18)$$

$$\hat{n} \cdot [\nabla \hat{C}_\pm^1 + z_\pm \hat{C}_\pm^0 \nabla \hat{\Phi}_1^1 + \hat{C}_\pm^1 \nabla \hat{\Phi}_1^0] = 0 \quad (19)$$

and at the far field,

$$\hat{\Phi}_1^1 = -\Phi_e / \Phi_T, \quad \hat{C}_\pm^1 = 0. \quad (20)$$

To perform the necessary analysis, we need to find the induced dipoles, and the polarizability of the particles. To extract the dipole moments and polarizability from the numerical solutions of the electric potential, we followed the method developed by Green and Jones.(Green and Jones 2006) The electric potential in the system results from the applied potential and the multipoles from the particle (Φ_p),

$$\Phi_t = \Phi_e + \Phi_p. \quad (21)$$

The potential due to the multipoles at a position R is given by the general expression,

$$\Phi_p = \sum_{n=1}^{\infty} \frac{p_n}{4\pi\varepsilon R^{n+1}} P_n(\cos\theta), \quad (22)$$

where p_n represent a multipole moment ($n = 1$ for a dipole, $n = 2$ for a quadrupole), while P_n denotes the Legendre polynomial of degree n . Multipoles up to the ninth order—can be extracted from the numerical solution of the potential by applying the orthogonality of the Legendre polynomials and the expression,

$$p_n = 4\pi\epsilon R_t^{n+1} \frac{2n+1}{2} \int_0^\pi \Phi_p(R_t) P_n(\cos\theta) \sin\theta d\theta. \quad (23)$$

$\Phi_p(R_t)$ is the electric potential due to the particle at a spherical surface of radius R_t . The spherical surface is centered on the particle, with R_t being several times its largest dimension. θ represents the polar angle in spherical coordinates. The integral provides a way to properly weight the orientation dependence for anisotropic particles. Φ_t stands for the value of the potential found by solving the Laplace and PNP equations in COMSOL. After every COMSOL simulation, the values of the total potential at R_t were extracted, and Φ_{R_t} was calculated through

$$\Phi_{p,R_t} = \Phi_t(R_t) - \Phi_e(R_t). \quad (24)$$

Subsequently, the dipole moments were calculated using Equation 23.

Aim1: Investigating the electric polarizability of metallocodielectric Janus spheres and ellipsoids in electrolyte solution

In the first step, **our main task is to find an efficient way to characterize the polarizability of particles**. Electrorotation can be an efficient tool for this purpose (Arcenegui et al. 2013b,a). In this technique, particles rotate due to an induced electrical torque. Electrical torque is balanced with viscous torque, which is a function of angular velocity. Hence, the angular velocity of the particle can be related to the polarizability and therefore to electrical properties of particle and the surrounding medium. Due to this relation, most studies investigate electrorotation spectrum (i.e. angular velocity vs frequency) to characterize the polarizability of particles (Keim et al. 2019).

In the electrorotation, two separate signals with the same voltage, but a phase difference of 90 degrees are applied to the electrodes. As illustrated in Figure 1A, the phase difference of signals generates rotating electric field between electrodes. When a particle is placed between electrodes, due to the difference in dielectric properties between the particle and the surrounding medium, a dipole is induced on the particle. When the direction of electric field changes, an electrical torque is exerted on the dipole to align itself with the electric field which causes the rotation of the particles. The direction of rotation depends on the dielectric properties of the particle and the medium. If the particle's response to change in the external electric field direction is faster than the surrounding medium (i.e. The particle is more polarizable than the medium), the particle's dipole is “ahead” of electric field. Therefore, it tries to “backtrack” the electric field leading to a negative torque. Since the torque is in the opposite direction of electric field, the particle shows counter-field rotation. On the other hand, if the medium is more polarizable than the particle, the electric field is ahead of the dipole, and the particle's dipole needs to “catch up” with the electric field, so a positive torque is applied on the dipole to align itself. Since the torque's direction is the same as external field, the particle will have co-field direction. Figure 1B summarizes counter-field and co-field rotations of particles in electrorotation.

In this aim, **our strategy is to use electrorotation and numerical simulation to see how changes in the particle and the medium will affect the polarizability**. The effect of these parameters on

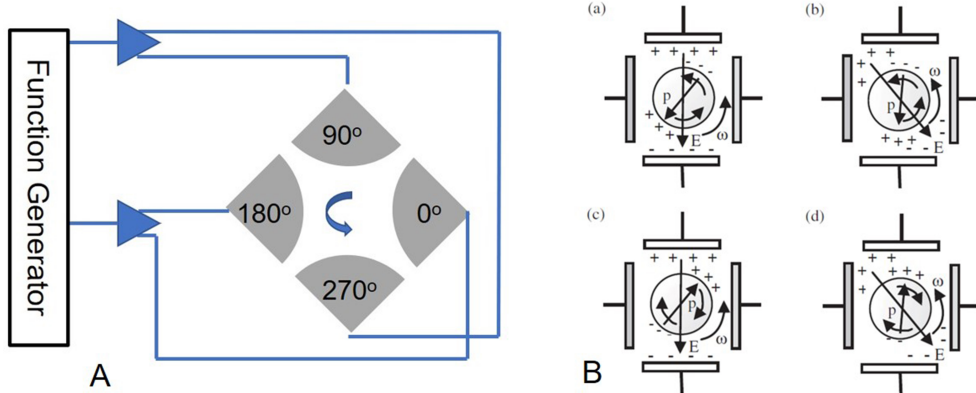


Fig. 1.—Rotation of a particle in a rotating electric field. A) Schematic of the electric circuit for electrorotation. Two channels with a phase difference of 90 degrees are required to develop the rotating field between electrodes. B) Rotation of particles due to the induced dipole on the particle. (a) and (b) cofield rotation: The medium is more polarizable than the particle and the dipole on the particle tries to catch up with the electric field. (c) and (d) counterfield rotation: The particle is more polarizable than the medium and the dipole backtracks to align itself with the electric field (Pethig 2017).

active motion, which will be tested in next steps, will elucidate whether active motion will follow the trends in the polarizability.

Method

To fabricate the electrorotation setup, 0.1 mm glass slides are utilized. The thickness of glass slide is important in the confocal microscopy for recording the motion of particles in the rotating electric field. Glass slides are cleaned and sonicated in three successive steps in acetone, isopropanol and water for 10 minutes in each step. After air drying the glass slides with nitrogen, glass slides are cleaned and treated with UV ozone. The fabrication includes two main steps. In the first step, negative photoresist technique is utilized. In this technique, the portion of the photoresist which is exposed to light remains insoluble and the rest of the photoresist is washed with the developer. For this technique, at first, a layer of NR9 is coated by using spin coater. The glass slide is then put on the hot plate (150 C) for about 2 minutes to make the layer stable. Subsequently, the glass slide is exposed to light (300 J/s) for 9 s to start the crosslinking process. The crosslinking process continues on the hot plate (100 C) for 90 seconds. After cooling down the glass slide, it is placed in the developer for 60 seconds. Finally, the patterned glass slide is rinsed with DI water to remove residuals. The final step of fabrication of the microfluidics setup, is to coat the glass slide with the gold by using Physical Vapour Deposition (PVD). To improve the adhesion of the gold to the glass slide, at first a 5-nm layer of titanium is coated on the glass and then a 75 nm thickness layer of gold is coated. After the deposition, a final treatment step is done in NMP solvent to remove the deposited gold on the areas other than the electrodes. Finally, the glass slides are rinsed with acetone and isopropanol and air-dried with nitrogen.

After JPs are fabricated, as explained above, JPs are tagged with fluorescent particles to help with JPs' motion visualization and angular velocity measurements. For this purpose, a suspension of 30

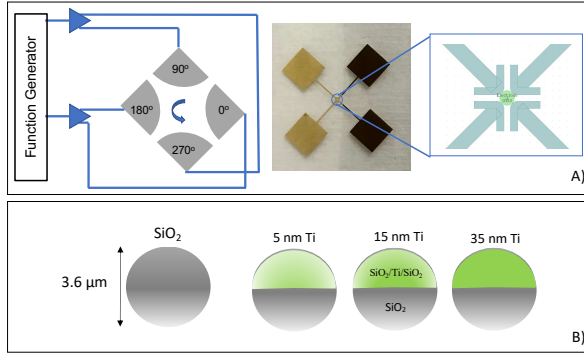


Fig. 2.—A) Setup to perform electrorotation measurements: application of rotating electric fields using a two-channel function generator and metal microelectrodes. B) The model systems are silica spheres of diameter of 3.66 μm , and JPs with additional layers of Ti and SiO₂.

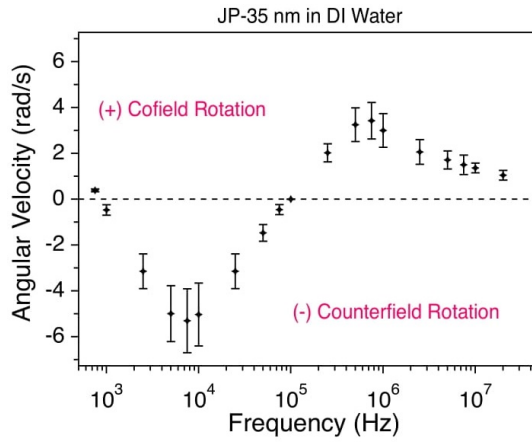


Fig. 3.—Electrorotation spectrum for Janus particles (JP-35 nm) in DI water shows two dipole relaxations, one centered at 7 kHz and the other at 100 kHz. Positive and negative values of angular velocity represent cofield and counterfield rotation, respectively. The applied potential was 6 V_{pp} .

μL of fluorescent PS, 600 μL NaCl solution and 300 μL of Janus particles are incubated for 2 hours. Then, successive centrifugation steps are performed to remove unbounded fluorescent particles and to replace the medium with DI water. Finally, the medium is changed to the target conductivity by sequential centrifuge- medium exchange cycles. The behavior of particles is observed in 3 salt concentrations (0.01 , 0.25 and 1 mM) with the medium conductivities of 0.5 , 5 and 14.6 mS/m. Then, as shown in figure 2B, particles are placed in the center of the region between electrodes by micropipettes. The angular velocity is measured by counting the number of complete revolutions of particles in a given time.

Results

As mentioned before, in the experiment, the focus is to find electrorotation spectrum (angular velocity vs frequency) and in the simulation, our goal is to find complex polarizability at different frequencies. The results for spherical JPs were published in *Soft Matter* (Behdani et al. 2021) and will be summarized in the current section.

Experimental Results-Electrorotation Spectrum of Silica and Janus Particles

We study the polarizability of Janus particles by measuring the angular velocity in a rotating field. Interaction of electric field with imaginary component of the induced dipole leads to asynchronous rotation of particles. Angular velocity at different frequencies for JP-35nm is presented in figure 3. For each frequency, each data point shows the average of 3 measurements of at least 3 particles. Error bars, representing standard deviation, shows the dispersion of data for each frequency. This dispersion originates from the change in the position of particles. At lower frequencies ($f < 100\text{kHz}$), the particles move in the opposite direction of the electric field's (counterfield rotation) showing that the induced dipole leads the electric field. In contrast, at higher frequencies ($f > 100\text{kHz}$), the particles rotate in the same direction of electric field (cofield rotation) which shows that electric field leads the induced dipole. For JP-35, electrorotation spectrum reaches a minimum at 7 kHz and a maximum at 100 kHz. This is a proof that the polarization is controlled by two different mechanisms.

Structure of JPs can also affect the interaction of the particle with the rotating field. In figure 4A, We investigated electrorotation of JPs with metal thicknesses of 35, 15 ,5 and 0 nm (silica). Silica particles show cofield rotation at all frequencies. For silica, the peaks for cofield rotation happens at around 10^6Hz , while there is an upturn in the angular velocity at frequencies below 10^5 . JP-5nm follows the same trend of cofield rotation at all frequencies with changes in the magnitude of angular velocity. However, further increase in the metal thickness will affect both direction and magnitude of the angular velocity. JP-15 nm and JP-35 nm show a combination of counterfield rotation at low frequencies ($f < 100\text{kHz}$) and cofield rotation at high frequencies ($f > 100\text{kHz}$). Although JP-15 and JP-35 show the same trend in the direction, the magnitude of angular velocity for JP-15 nm is significantly lower than JP-35 nm's (about half).

To find the effect of the medium conductivity, we study the electrorotation of JP35 at 0.5, 5 and 14.6 mS/m. Figure 4B shows that by increasing the conductivity, three main changes are observed : First, cofields and counterfield peaks shift to higher frequencies. For instance, counterfield peaks occur at 20 kHz for 0.5 mS/m and 100 kHz for 14.6 mS/m. Second, the peak velocities for cofield and counterfields rotations decrease significantly. For instance, the peak angular velocity decreases to half by changing the medium from DI water to NaCl solution of 0.5 mS/m. Third, cofield peak disappears at very high conductivities. At 14.6 mS/m, JP-35 only shows a single counterfield peak. The findings show that the medium conductivity can significantly change both the direction and the magnitude of angular velocity. Therefore, conductivity can play an important role in tuning polarizability of JPs.

Our experimental investigation shows that there are two competing charge relaxations which govern electrorotation of JPs. The first relaxation (counterfield peak) can be related to the metal component of JPs while the second one (cofield peak) can be attributed to the dielectric core and outer layer. Moreover, the structure of JPs and medium conductivity can significantly affect the polarizability of JPs in the electrolyte solution. In the next step, we solve PNP equation to get more mechanistic insights about the polarization of Janus particles.

Mechanistic Insight into the Polarization of JPs

For efficient particle manipulation in AC field, we need to attain full control on the polarizability. **Numerical simulation can help us understand the governing physics behind the polarization of particles. By understanding these physics, we can adjust and tune different process**

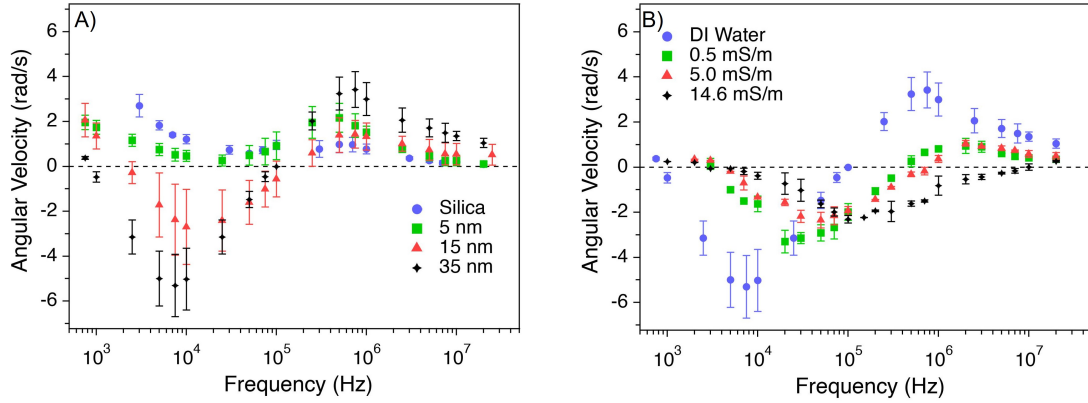


Fig. 4.—A) Thickness of metallic layer determines the counterfield rotation of Janus particles (JPs). As the thickness of titanium decreases from 35 nm to 0, rotation at low frequencies transition from counterfield to cofield. B) Conductivity of the medium strongly affect the electrorotation spectra of JP-35nm particles. The angular velocity was measured for JP-35 nm suspended in DI water and NaCl solutions of different conductivities (0.5, 5.0 and 14.6 mS/m). The applied potential was 6 V_{pp}.

parameters in the system to achieve active motion of particles in a predefined direction. In the simulation, we assumed that the metal layer is perpendicular to the electric field. With this assumption, 3D simulation is not necessary, and the computational load will decrease significantly. Figure 5A shows the Im(B) of JP-35 in 0.01 mM NaCl solution. It shows two peaks, corresponding to counterfield and cofield peaks in the electrorotation according to equation 3. The frequency for the first peak is similar to the experiment's while the second peak' frequency shows deviation from experimental value. The model confirms that polarization of JPs occurs due to two different relaxation mechanisms.

The first peak is controlled by charging of the double layer, as depicted in 5B . In this mechanism, at low frequencies, ions do have enough time to form the induced double layer around the particle and the double layer is fully charged while at very high frequencies, there is negligible induced charge in the double layer . Therefore, there is a frequency at which the induced double layer cannot keep up with the applied field . This frequency is called RC frequency and calculated by $f_{RC} = \lambda\sigma/a\epsilon$ where σ , λ , ϵ are bulk conductivity, Debye length and permittivity, respectively . Since this behavior is observed for fully metal particles (Ren et al. 2011), we can conclude that the metal layer determines the counterfield peak.

The second peak is controlled by Maxwell-Wagner (MW) interfacial polarization. In this mechanism, the polarization of particles is due to the difference in the conductivity and permittivity of the particle and medium (García-Sánchez et al. 2019). The relaxation time for MW interfacial polarization can be calculated as $(\tau_{MW} = \frac{\epsilon_p + 2\epsilon_m}{\sigma_p + 2\sigma_m})$. In general, the relaxation time for CDL is much higher than the MW interfacial polarization as CDL deals with the ion transport. For JPs, interfacial polarization happens at around 1000 kHz. Figure 6A shows the Im(K) of silica particles at different zeta potentials. The peak frequency is approximately the same as the cofield peak for JPs. Although the peak frequency remains the same, the zeta potential can significantly change the sign of Im(K). A non-charged silica particle shows a positive peak , corresponding a counterfield rotation. By decreasing the zeta potential, the Im(K) 's value decreases and for higher zeta potential (> -40), the Im(K) turns to negative, which corresponds the cofield rotation. In the experiment,

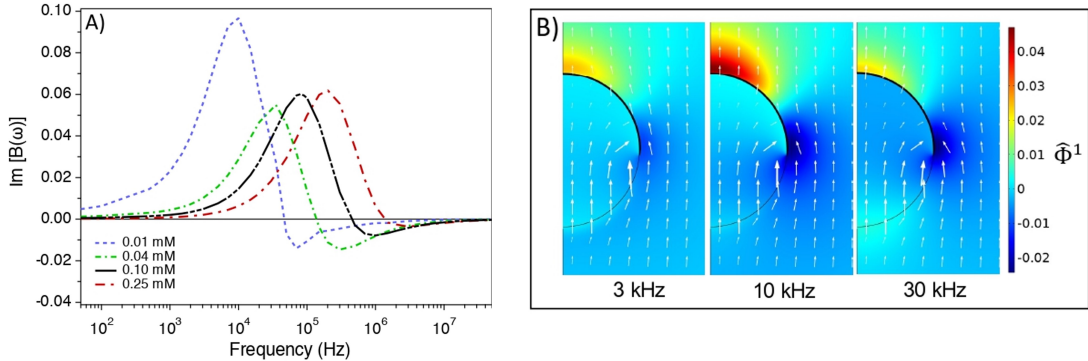


Fig. 5.—The electrokinetic model reproduces the two relaxations observed in electrorotation experiments. A) Magnitude of the imaginary part of the dimensionless polarizability, calculated from the electrokinetic model for JP-35 nm, with $\zeta = -60$ mV and $r = 1.8 \mu\text{m}$. The calculation was performed using the diffusivity values for NaCl, at similar concentrations as in the experiments. Notice that a positive dipole term implies counterfield rotation, according to Equation 3. B) Heat and vector maps representing the complex part of the scaled potential and electric field for JP-35nm in 0.01 mM NaCl, at different frequencies.

silica particles show cofield rotation, proving that we cannot capture the polarization of JPs and silica without consideration of surface charge. Figure 6B shows that with the increase in the salt concentration, relaxation happens at higher frequencies while the negative value decreases and in very high concentrations, the negative value turns into positive. In the experiment, for silica and Janus particles, it was observed that at high salt concentrations, cofield rotation disappears and counterfield rotation with very low angular velocity values emerges. This provides further proof that the second relaxation for JPs is governed by the combination of the surface charge and the interfacial polarization.

While the model can capture cofield and counterfield peaks, it cannot show cofield rotation at low frequencies ($f < 1\text{kHz}$). At low frequencies, the electroosmosis flow originates from the interaction of field and charged double layer around the particle (Beltramo and Furst 2012) and the flow cannot be justified merely with balance of the electrical and viscous torque in the current model. The other limitation of the current simulation is neglecting other orientation of metal layer (parallel to electric field) which might be significant especially at higher frequencies.

Current experimental and modeling studies provide insights about the polarization of JPs which can be used in the design and fabrication of reconfigurable systems. Results show that the first relaxation is governed by the metal and the second relaxation is governed by dielectric core and outer layer. According to the results, the structure of particles, medium conductivities and surface charge of particles can affect polarizability and the motion of particles. These parameters can be utilized to tune the response of particles to electric field.

Proposed Research Plan

3D simulation of response of particles to the AC field

In our study, we focused on the perpendicular orientation of the particle (perpendicular to electric field) to decrease the computational load and to solve a symmetric problem in 2D. This assumption causes deviations from experimental results, especially at higher frequencies. **To find the effect of orientation of particles on their polarizability in the system, we plan to develop a 3D model for spherical JPs.** Also, it should be noted that 3D simulation will be helpful for next steps of

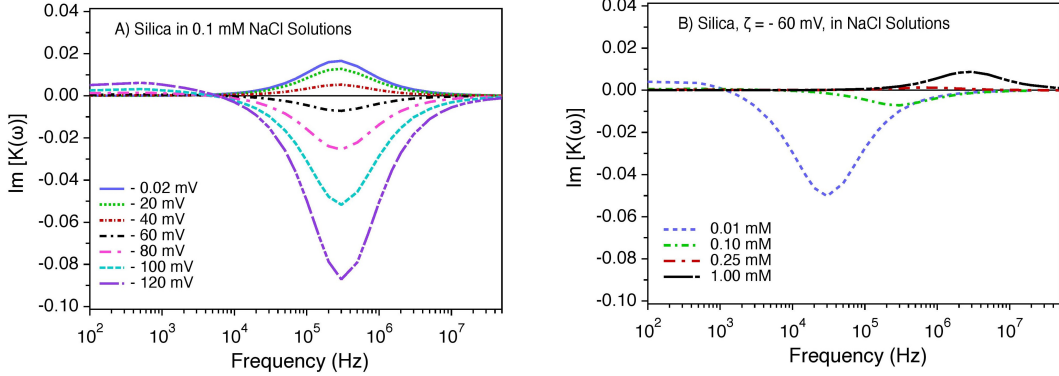


Fig. 6.—Magnitude of the imaginary part of the dipole coefficient, calculated from the electrokinetic model for a silica particle with $r = 1.8 \mu\text{m}$. The calculation was performed using the diffusivity values for NaCl at similar concentrations as in the experiments. Notice that a negative dipole term implies cofield rotation, according to Equation 3. A) Results for different values of ζ in 0.1 mM NaCl. B) Results for different values of NaCl concentration, with $\zeta = -60 \text{ mV}$.

the project to track the propulsion of particles in the whole domain and to account for the dipolar interaction of particles on each other.

Finding electrical polarizability of metalldielectric Janus Ellipsoids in electrolyte solutions.

In biomedical application, particles deviate from a spherical geometry. This deviation affects their propulsion and collective dynamics. Since in our hypothesis, active motion is correlated to the polarizability, we plan to find electrical polarizability of non-spherical particles. For this purpose, we chose Janus ellipsoids whose geometry is distinct from the more commonly studied case of Janus spheres. In our proposal, **we want to perform electrorotation measurements of dielectric and Janus ellipsoids and conduct a 3D modeling on their polarizability.** This will help us achieve a clear picture about the polarizability of these particles and to apply this information to achieve successful active motion of non-spherical particles. It is important to highlight that, for future applications of JPs in cargo transport, the ellipsoids are more favorable than spheres as they can transport more particles.

Aim2 : Engineering self propulsion of particles through the manipulation of polarizability.

Active particles absorb the external energy, stored in the surrounding medium, and move like microorganisms (e.g. Bacteria and algae) in the medium (Wu et al. 2020). They have been used in single cell analysis, drug delivery, detoxification , remote surgery and self healing systems (Lee et al. 2019). For successful propulsion, developing efficient strategies for local control and self-orientation of microparticles are vital. Most of these strategies can be classified in two categories. In the first category, complicated microchannels are designed and fabricated to steer the particle. However, still the interaction of particles and the walls is very complicated to understand. In the second category, an external field is used to navigate the particles. Magnetic fields and light sources are popular approaches to enforce a local gradient around the particle and so self propulsion of particles. One drawback in these strategies is that constant manual or automatic interference is

required to direct the particle in the predefined route (Boymelgreen et al. 2016).

For active Janus particles, electric fields are often used to control the self propulsion. Previous works in the literature show successful applications of these colloidal systems for electroporation of bacteria and cargo transport. The advantage of using an electric field in these systems is the simplicity of the process as the controlling factor is only the frequency of the external field. To interpret these propulsion systems, an understanding of the polarizability of particles inside the field is needed. Although there are several hypotheses, proposed for the effect of polarizability on the self-propulsion, there is no consensus on the explanation of self-propulsion and its dependence on polarizability. Our study can shed light on this gap in the literature. The results of our study can help us achieve more efficient particle manipulation in the artificial active systems.

In aim one, we characterize the polarizability of the particles and find the effect of particle's structure and medium on the polarizability. **In this part of the project, we examine the propulsion of particles in the same conditions and try to map the information from polarizability to the propulsion.** This will help us extract the effect of polarizability on the polarization and explain the propulsion behavior of particles.

Method

To achieve this aim, we place JPs inside a non-rotating electric field. JPs with metal thicknesses of 5, 15 and 35 nm were used. Similar to the electrorotation experiment, medium has three different conductivities of 0.5, 5 and 14.6 mS/m. To place particles in the medium with the target conductivity, consecutive cycles of centrifugation-medium exchange were used. The experimental setup is built by confining approximately 20 μ L of the suspension between two ITO slides separated by 120 micron- dielectric spacer. The ITO slides are previously cleaned by sonicating in acetone, isopropanol and DI water for 10 minutes in each medium. After sonication, slides are treated with UV ozone for 10 minutes and placed in polymer solution for 30 minutes to prevent attachment of particles to the surface. The conductive slides are connected to a function generator which can make an AC electric field with frequencies between 1 kHz-20 MHz. For measurements, potential amplitude is set at 10 Vpp. The propulsion of JPs was captured by Leica TCS SP8 with 20x, 0.75NA , air objective. Particles are excited with 488nm lasers and particle's motion is captured with 14.7 frame/s.Fiji is utilized to extract particle trajectory and mean square displacement (MSD) of particles.

Propulsion velocity of particle can be calculated by fitting MSD to the following equation introduced by Howse et al (Howse et al. 2007).

$$\langle \Delta L \rangle^2 = 4D\Delta t + \frac{v^2\tau_R^2}{2} \left[\frac{2\Delta t}{\tau_R} + e^{-\frac{2\Delta t}{\tau_R}} - 1 \right] \quad (25)$$

where v , D and τ_R are propulsion velocity, diffusion constant and rotational time constant ($\tau_R = \frac{8\pi\mu^3}{k_B T}$). In the equation 25, first term represents the motion due to the Brownian motion and the second terms shows propulsion of the particles.

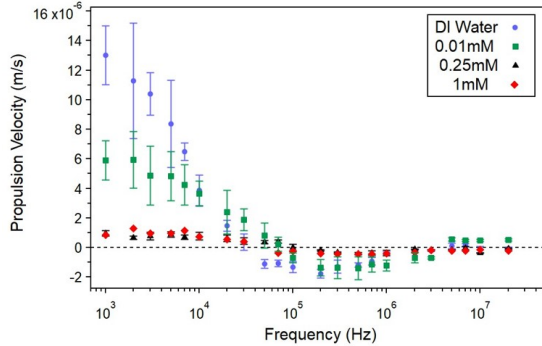


Fig. 7.—Self propulsion of JP35 at different conductivities. In the plot, positive values show the propulsion with silica side heading forward and negative values present the propulsion with metal cap heading forward. By increasing the conductivity, the peak velocity decreases, and the peak shifts to the higher frequencies.

Preliminary Results

Figure 7 shows the propulsion velocity of JP-35nm at different frequencies of AC field. For each frequency, at least 5 measurements were performed, and error bars show the standard deviation of measurements. The scattering in data may originate from the interaction of adjacent dipoles on the particles. This interaction is more significant at lower frequencies since particles have higher velocities and they might pass each other. As shown in Figure 7, at low frequencies ($f < 10^5$), the particle moves with silica heading forward (positive velocity) while at higher frequencies ($f > 10^5$), propulsion's direction reverses and the metal cap heads forward (negative velocity).

To understand the effect of the conductivity, the propulsion velocity of JP-35 in DI water and three salt solutions (0.01, 0.25 and 1mM) was measured , as illustrated in figure 7. By increasing the conductivity, two important observations were found. First, by increasing the conductivity, the peak velocity decreases. Second, the peak frequency will shift to higher frequencies by increasing the conductivity.

Although complete study of the effect of metal thickness and effect of conductivity in other thicknesses are yet to be performed, current results provide evidence that polarizability controls the propulsion of particles. First, the effect of conductivity on the propulsion velocity and angular velocity in the electrorotation is similar. More importantly, both phenomena follow the same trend. Kronig-Krammer relations show that the complex and real parts of polarizability are correlated : At frequencies, where real part experiences high gradient, the imaginary component experiences a peak (Garcia-Sanchez et al. 2012). Comparison of self propulsion and electrorotation spectrum of JP-35 in water shows that in the areas that propulsion is experiencing high gradient, the electrorotation experiences a peak. Since we showed that the electrorotation is governed by complex polarizability , **we can infer that propulsion is controlled by the real part of polarizability**. While promising, further experiments can provide more insight about the system and the dependence of propulsion to real part of polarizability.

Proposed Research Plan

Finding effect of metal thickness and the medium conductivity on self propulsion

Preliminary results suggest that self-propulsion of particles is governed by the real component of polarizability. **In this study, we will measure the effect of the medium and particle's structure**

on the propulsion. Key parameters for this study are medium conductivity and the metal thickness of JPs. Since the effect of these parameters were already investigated in electrorotation, we can test whether self-propulsion can be tuned by adjusting the polarizability of the particles. **We also plan to perform a 3D numerical simulation to better understand the propulsion of JPs.** The model will couple PNP equation with momentum and continuity equations to find the velocity of JPs inside an AC field. Our final goal is to gain full control on the propulsion velocity and direction by engineering polarizability of particles.

Aim3 : Controlling collective dynamics of Janus Particles in AC field

Programming nonequilibrium interactions by adjusting polarizability is not limited to the self-propulsion of a single particle. Controlling collective dynamics and transport properties are applicable to particle transport and mixing in microfluidics (Zhang et al. 2017, Colen et al. 2021, Elkeles et al. 2020). In these systems, the interaction of particles with each other and the domain boundaries become important. Despite its significance, the effect of particle's concentration and geometric confinement in active systems has rarely been studied before. In this part of the project, we plan to develop strategies to control the non equilibrium interaction of active colloids. Particularly, we want to investigate the effect of these non-equilibrium interactions on the collective behavior of active Janus particles and how we can program these interactions. Previously, we observed that the structure of JPs and the medium conductivity can affect polarizability and self propulsion of JPs. Our hypothesis is that the same parameters can be used to program collective dynamics of these colloidal systems. To test our hypothesis, **we investigate the collective dynamics of JPs in two conditions: in high concentration of particles and under geometric confinement.** Our main goal is to predict the behavior of particles in more realistic environments (e.g., porous media or tissue) and to find future applications for active particles in biomedical systems.

Proposed Research Plan

Collective dynamics of active particle in high concentration suspension

We will probe the nature and consequences of multi-body interactions by changing the surface concentration of particles and consequently, the interparticle distance. We will increase the concentration of Janus particles in the suspension to 90%, in contrast to 0.5-1% in our previous studies, to see how collective dynamics of particles will change. By increasing the concentration, both adjacent dipoles and external field will affect the dipole on the particle. The particles will be fabricated as explained before. We will measure the rotational and translation velocities under different strengths of dipole-dipole interactions. Our final goal is to attain a full control on the motion of particles in AC fields in all levels.

Collective dynamics of active particles under confinement

Design and fabrication of microrobots depend on their performance in real environments such as porous media and tissues. In order to understand principle of transport under these conditions and develop strategies to control the collective dynamics of particles, it is required that as many scenarios where the particles experience the confinement are developed. **To achieve this goal, we will handle the plan in two scenarios. In the first scenario, particles will be placed in the interface of oil and water.** Difference in the density and dielectric properties between the

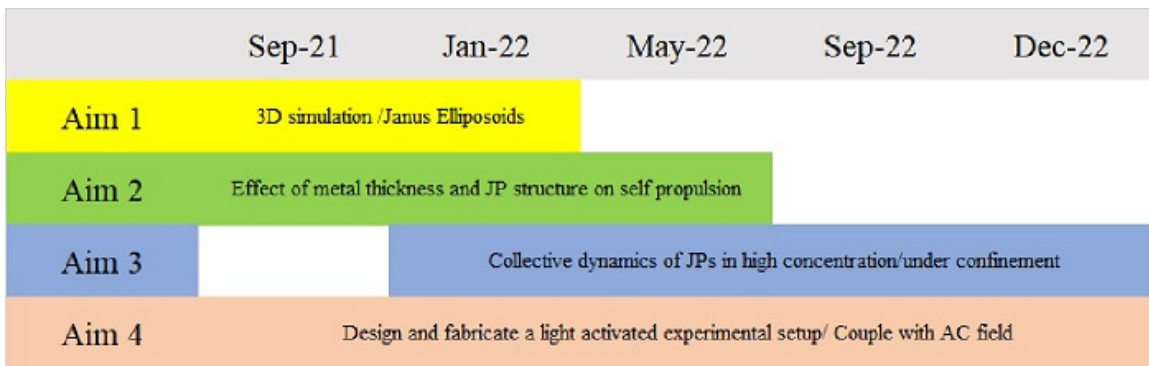


Fig. 8.—Timeline of proposed research.

particle and two media will lead to a buoyancy-electrohydrodynamic flow and a complex collective dynamics of particles. **In the second scenario, geometry and dimension of the device will change to see how it will affect the active motion and collective dynamics of particles in a more realistic domain.**

Aim 4: Light driven motion of self propelled Janus particles in the presence of AC field

Light driven motion is a new and promising approach for propulsion of artificial active colloids. In this approach, the surface of the particle is covered by photo-active chemicals. UV light will provide the activation energy to initiate the reaction. The consumed and produced species during the reaction causes a local gradient around the particle, leading to the propulsion of particles. The reactions may involve hydrolysis (Holterhoff et al. 2020), photo-switchable molecules (Feldmann et al. 2019) or functional groups on the surface of particles (Huang et al. 2021). To increase the propulsion velocity in these systems, AC electric fields can be utilized. Applying AC field can increase the controllability of the process as it decreases the degree of freedom in the system. Recently, there have been several works on the light driven self propulsion in the literature, however, to the best of our knowledge, no study has been performed on the simultaneous use of electric field and UV light to navigate microrobots. To fill the gap, in this aim, **we will use AC field and light sources to achieve self-propulsion and control collective dynamics of JPs.** Our final goal is to achieve better control on steering of active colloids in biomedical systems.

To achieve the goal of this aim, we will explore a suitable photo-activated reaction. Based on the reaction mechanism, we can determine wavelength and intensity of the light, the medium, the particle and the fabrication approach. In the first stage, we will develop active motion by using only light source and then, AC field will be coupled with the light source to tune the active motion of particles.

Timeline of proposed work

Figure 8 shows the timeline to complete proposed research work in the project.

References

- Juan J Arcenegui, Pablo García-Sánchez, Hywel Morgan, and Antonio Ramos. Electric-field-induced rotation of Brownian metal nanowires. *Physical Review E*, 88(3):33025, 2013a.
- Juan J Arcenegui, Antonio Ramos, Pablo García-Sánchez, and Hywel Morgan. Electrorotation of titanium microspheres. *Electrophoresis*, 34(7):979–986, 2013b. ISSN 0173-0835.
- Behrouz Behdani, Kun Wang, and Carlos A Silvera Batista. Electric Polarizability of Metallodielectric Janus Particles in Electrolyte Solutions. *Soft Matter*, 2021.
- Peter J Beltramo and Eric M Furst. Transition from dilute to concentrated electrokinetic behavior in the dielectric spectra of a colloidal suspension. *Langmuir*, 28(29):10703–10712, 2012. ISSN 0743-7463.
- Alicia Boymelgreen, Gilad Yossifon, and Touvia Miloh. Propulsion of active colloids by self-induced field gradients. *Langmuir*, 32(37):9540–9547, 2016. ISSN 0743-7463.
- Alicia M Boymelgreen, Tov Balli, Touvia Miloh, and Gilad Yossifon. Mobile Microelectrodes: Towards active spatio-temporal control of the electric field and selective cargo assembly. *arXiv preprint arXiv:1708.02228*, 2017.
- Alicia M. Boymelgreen, Tov Balli, Touvia Miloh, and Gilad Yossifon. Active colloids as mobile microelectrodes for unified label-free selective cargo transport. *Nature Communications*, 9(1):1–8, 2018. ISSN 20411723. doi: 10.1038/s41467-018-03086-2. URL <http://dx.doi.org/10.1038/s41467-018-03086-2>.
- Yu-Liang Chen, Cheng-Xiang Yang, and Hong-Ren Jiang. Electrically enhanced self-thermophoresis of laser-heated Janus particles under a rotating electric field. *Scientific reports*, 8(1):1–7, 2018. ISSN 2045-2322.
- Udit Choudhury, Arthur V. Straube, Peer Fischer, John G. Gibbs, and Felix Höfling. Active colloidal propulsion over a crystalline surface. *New Journal of Physics*, 19(12), 2017. ISSN 13672630. doi: 10.1088/1367-2630/aa9b4b.
- Jonathan Colen, Ming Han, Rui Zhang, Steven A Redford, Linnea M Lemma, and Link Morgan. Machine learning active-nematic hydrodynamics. 2021. doi: 10.1073/pnas.2016708118/-DCSupplemental.y.
- Ahmet F Demirörs, Mehmet Tolga Akan, Erik Poloni, and André R Studart. Active cargo transport with Janus colloidal shuttles using electric and magnetic fields. *Soft Matter*, 14(23):4741–4749, 2018.
- Tom Elkeles, Pablo Garcia-Sánchez, Wu Yue, Antonio Ramos, and Gilad Yossifon. Dielectrophoretic equilibrium of complex particles. *MicroTAS 2020 - 24th International Conference on Miniaturized Systems for Chemistry and Life Sciences*, pages 40–41, 2020.
- David Feldmann, Pooja Arya, Nino Lomadze, Alexey Kopyshev, and Svetlana Santer. Light-driven motion of self-propelled porous Janus particles. *Applied Physics Letters*, 115(26):263701, 2019. ISSN 0003-6951.
- Pablo Garcia-Sánchez, Yukun Ren, Juan J Arcenegui, Hywel Morgan, and Antonio Ramos. Alternating current electrokinetic properties of gold-coated microspheres. *Langmuir*, 28(39):13861–13870, 2012. ISSN 0743-7463.
- Pablo García-Sánchez, Jose Eladio Flores-Mena, and Antonio Ramos. Modeling the AC electrokinetic behavior of semiconducting spheres. *Micromachines*, 10(2):100, 2019.
- Nicolas G Green and Thomas B Jones. Numerical determination of the effective moments of non-spherical particles. *Journal of Physics D: Applied Physics*, 40(1):78, 2006. ISSN 0022-3727.
- Andrew Leeth Holterhoff, Victoria Girgis, and John G Gibbs. Material-dependent performance of fuel-free, light-activated, self-propelling colloids. *Chemical Communications*, 56(29):4082–4085, 2020.
- Jonathan R Howse, Richard A L Jones, Anthony J Ryan, Tim Gough, Reza Vafabakhsh, and Ramin Golestanian. Self-motile colloidal particles: from directed propulsion to random walk. *Physical review letters*, 99(4):48102, 2007.
- Tao Huang, Bergoi Ibarlucea, Anja Caspari, Alla Synytska, Gianaurelio Cuniberti, Joost de Graaf, and Larysa Baraban. Impact of surface charge on the motion of light-activated Janus micromotors. *The European Physical Journal E*, 44(3):1–11, 2021. ISSN 1292-895X.

- Kevin Keim, Mohamed Z Rashed, Samuel C Kilchenmann, Aurélien Delattre, António F Gonçalves, Paul Éry, and Carlotta Guiducci. On-chip technology for single-cell arraying, electrorotation-based analysis and selective release. *Electrophoresis*, 40(14):1830–1838, 2019. ISSN 0173-0835.
- Jin Gyun Lee, Allan M. Brooks, William A. Shelton, Kyle J.M. Bishop, and Bhuvnesh Bharti. Directed propulsion of spherical particles along three dimensional helical trajectories. *Nature Communications*, 10(1):1–8, 2019. ISSN 20411723. doi: 10.1038/s41467-019-10579-1. URL <http://dx.doi.org/10.1038/s41467-019-10579-1>.
- Touvia Miloh and Jacob Nagler. Electrorotation of leaky-dielectric and conducting microspheres in asymmetric electrolytes and angular velocity reversal. *Electrophoresis*, 41(15):1296–1307, 2020. ISSN 15222683. doi: 10.1002/elps.201900478.
- Ran Niu and Thomas Palberg. Modular approach to microswimming. *Soft Matter*, 14(37):7554–7568, 2018. ISSN 17446848. doi: 10.1039/c8sm00995c.
- Sinwook Park, Lior Finkelman, and Gilad Yossifon. Enhanced cargo loading of electrically powered metallo-dielectric pollen bearing multiple dielectrophoretic traps. *Journal of Colloid and Interface Science*, 588:611–618, 2021. ISSN 0021-9797.
- Ronald R Pethig. *Dielectrophoresis: Theory, methodology and biological applications*. John Wiley & Sons, 2017. ISBN 1118671457.
- Yu K Ren, Diego Morganti, Hong Y Jiang, Antonio Ramos, and Hywel Morgan. Electrorotation of metallic microspheres. *Langmuir*, 27(6):2128–2131, 2011. ISSN 0743-7463.
- C. Wyatt Shields and Orlin D. Velev. The Evolution of Active Particles: Toward Externally Powered Self-Propelling and Self-Reconfiguring Particle Systems. *Chem*, 3(4):539–559, 2017. ISSN 24519294. doi: 10.1016/j.chempr.2017.09.006.
- Sho C. Takatori and John F. Brady. Forces, stresses and the thermodynamics of active matter. *Current Opinion in Colloid and Interface Science*, 21:24–33, 2016. ISSN 18790399. doi: 10.1016/j.cocis.2015.12.003. URL <https://doi.org/10.1016/j.cocis.2015.12.003>.
- Andreas Walther and Axel H E Müller. Janus particles. *Soft Matter*, 4(4):663–668, 2008.
- Yue Wu, Afu Fu, and Gilad Yossifon. Active particles as mobile microelectrodes for selective bacteria electroporation and transport. *Science advances*, 6(5):eaay4412, 2020. ISSN 2375-2548.
- Jie Zhang, Erik Luijten, Bartosz A. Grzybowski, and Steve Granick. Active colloids with collective mobility status and research opportunities. *Chemical Society Reviews*, 46(18):5551–5569, 2017. ISSN 14604744. doi: 10.1039/c7cs00461c.
- Hui Zhao. Double-layer polarization of a non-conducting particle in an alternating current field with applications to dielectrophoresis, sep 2011. ISSN 01730835. URL <https://pubmed.ncbi.nlm.nih.gov.proxy.library.vanderbilt.edu/21823130/>.